THE JOURNAL OF PHYSICAL CHEMISTRY B

Article

pubs.acs.org/JPCB

Molecular Binding Behaviors between Tetrasulfonated Bis(*m*-phenylene)-26-crown-8 and Bispyridinium Guests in Aqueous Solution

Ling Chen, Ying-Ming Zhang, and Yu Liu*

Department of Chemistry, State Key Laboratory of Elemento-Organic Chemistry, Nankai University, Tianjin 300071, People's Republic of China

Supporting Information

ABSTRACT: A highly water-soluble crown ether bearing four sulfonate groups (**1**) was synthesized by sulfonation of neutral bis(*m*-phenylene)-26-crown-8. The complexation behavior of **1** with two bispyridinium-based guests, methyl viologen (MV^{2+}) and 1,2-bis(pyridinium)ethane (BPE^{2+}), was systematically investigated in both aqueous solution and the solid state by ^1H NMR spectroscopy, crystallography, and microcalorimetry. The crystallographic studies of superstructures $MV^{2+}\subset$**1** and $BPE^{2+}\subset$**1** show that MV^{2+} forms an interpenetrated complex with **1**, and conversely, BPE^{2+} is bound outside the cavity of **1** as an electrostatic complex. Furthermore, microcalorimetric titration reveals the thermodynamic origins of this different binding process; that is, MV^{2+} threads through the cavity of **1** with a significant enthalpy change, while BPE^{2+} mainly associates with the sulfonate groups of **1**, accompanied by a dominant entropy change. The obtained results demonstrate a structure-dependent binding process in complexes $MV^{2+}\subset$**1** and $BPE^{2+}\subset$**1**, depending on the relative locations of positive charges on nitrogen atoms and the bridge linkers between two pyridinium moieties in the guest molecules.

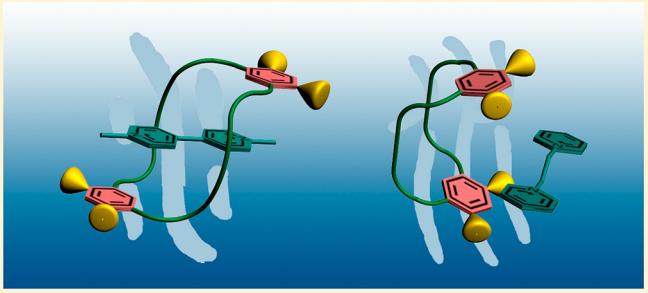

INTRODUCTION

The rational design and construction of multidimensional nanoarchitectures based on crown ether derivatives have recently stimulated an upsurge of interest, mainly due to their obvious advantages to form the sophisticated topological features[1] of mechanically interlocked complexes with photo- and electroactive functionalities.[2] Up to now, great progress has been made in exploring crown ether-based artificial systems, including chiral recognition, molecular switches, chemical sensors, and ion channels,[3] by using their selective complexation behaviors toward inorganic/organic cations, such as metal ions,[4] alkyl ammonium,[5] and viologen.[6] However, despite the fact that crown ethers as a class of synthetic receptors have been known and developed for several decades, the inventive applications of its water-soluble derivatives have thus far been essentially ignored and limited. The modified crown ethers with high water solubility are scarcely exploited as a building block to fabricate the tailor-made multicomponent assemblies in supramolecular chemistry. To the best of our knowledge, only a few examples of stability constants and binding behaviors involving the complexation of crown ethers and organic cations have been experimentally studied in aqueous media.[7] For instance, Tiburcio and Loeb et al. have devised a [2]-pseudorotaxane system comprised of negatively charged dibenzo[24]-crown-8 with sulfonate groups as a wheel and positively charged 1,2-bis(pyridinium)ethane as an axle, implementing the cooperative ion−ion interactions in the formation of stable threaded inclusions.[8] Moreover, with the introduction of anionic substituents into bis-*p*-phenylene-34-crown-10, a series of electroneutral zwitterion-like host−guest complexes were successfully constructed, exhibiting bispyridinium-based [2]pseudorotaxanes and [2]rotaxanes in various solvents.[9]

In the wake of these fascinating results and inspired by our ongoing interest concerning the molecular recognition and thermodynamic investigation on water-soluble macrocycles of cyclodextrin,[10] *p*-sulfonatocalixarene,[11] and cucurbituril,[12] herein we would like to report a novel tetrasulfonated crown ether (**1**) capable of effectively binding two bispyridinium derivatives, methyl viologen (MV^{2+}) and 1,2-bis(pyridinium)ethane (BPE^{2+}), through noncovalent multiple interactions in water, which is strikingly distinctive from the reported results in organic solution. The crystallographic studies and microcalorimetric titrations reveal that the combination of ion−dipole, hydrogen-bonding interconnection, and $\pi-\pi$ stacking interactions jointly stabilize the electrically interpenetrated structure of $MV^{2+}\subset$**1**, and the strongly entropy-driven process indicates that electrostatic attraction between the negatively charged crown ether and positively charged bispyridinium units is the decisive driving force in the electrostatic complex of $BPE^{2+}\subset$**1**. This unexpected binding process in the present

Received: June 5, 2012
Published: July 18, 2012

   dx.doi.org/10.1021/jp305503e | *J. Phys. Chem. B* 2012, 116, 9500−9506

Scheme 1. Syntheses of 1 and the Molecular Structure of Guests

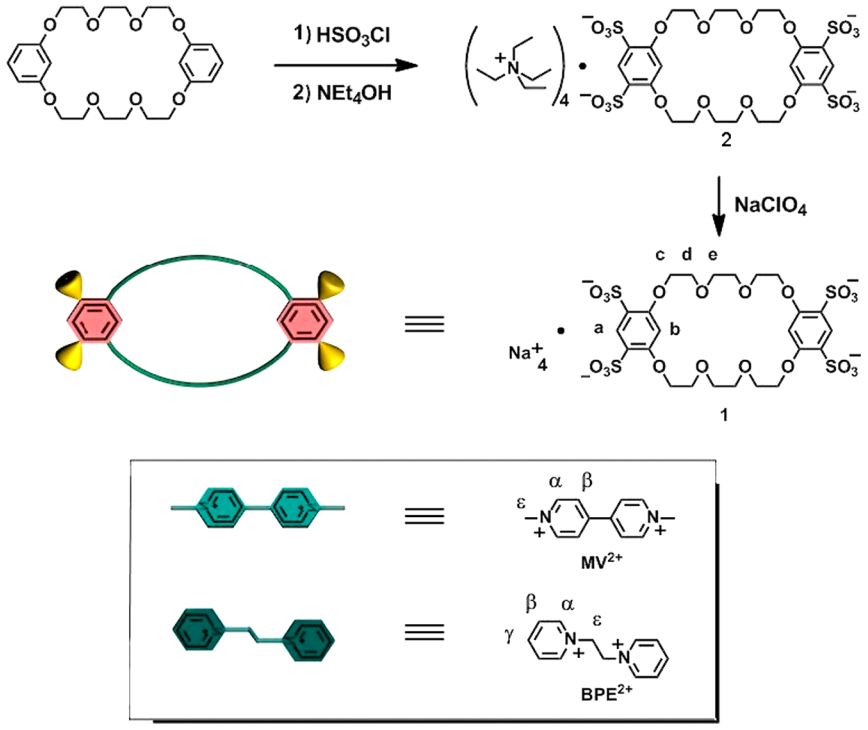

research will serve to promote our understanding of this important, but less investigated, area of functionalized supramolecular assemblies.

RESULTS AND DISCUSSION

Synthesis of Anionic Crown Ether 1. The synthetic route of tetrasulfonated crown ether **1** is depicted in Scheme 1. Bis(*m*-phenylene)-26-crown-8 (BMP26C8) was prepared by a modified literature procedure.[13] Then, the precursor BMP26C8 was reacted with chlorosulfonic acid and neutralized with a tetraethylammonium hydroxide solution in mild condition to afford tetraethylammonium salt (**2**).[14] Followed by the counterion exchange in acetonitrile, sodium salt **1** has a satisfactory solubility up to 100 mM in water (i.e., 85.6 mg/mL). Moreover, two of the most commonly employed model guests with different positively charged positions, methyl viologen (MV^{2+}) and 1,2-bis(pyridinium)ethane (BPE^{2+}),[6,15] were chosen to comprehensively study the significance of cooperative noncovalent interactions in supramolecular architectures.

NMR Titration. The quantitative investigation of intermolecular complexation of water-soluble crown ether **1** with two bispyridinium derivatives, MV^{2+} and BPE^{2+}, was conducted by means of ^{1}H NMR titration in D_2O. The chemical shift changes ($\Delta\delta$) of guests MV^{2+} and BPE^{2+} upon their complexation with host **1** are listed in Table S1 of the Supporting Information. As discerned from Figure 1, the chemical shifts of two complexes ($MV^{2+}\subset$**1** and $BPE^{2+}\subset$**1**) are consistent with the formation of "fast exchange" equilibrium. The corresponding $\Delta\delta$ values take on similar characteristics in the complexes $MV^{2+}\subset$**1** and $BPE^{2+}\subset$**1**; that is, all of the aromatic protons of both **1** (H_a and H_b) and two guests (H_α, H_β, and H_ε) underwent a small complex-induced upfield shift, and the ones of ethylene glycol chains of **1** (H_d and H_e) exhibited a slight downfield shift in the presence of guest

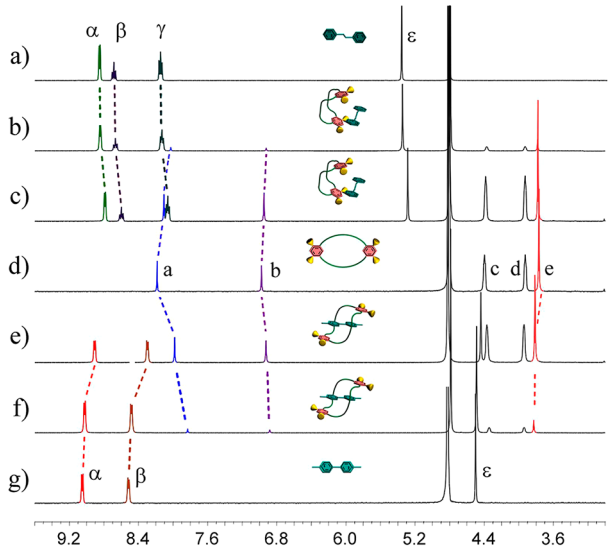

Figure 1. Partial ^{1}H NMR spectra (400 MHz, D_2O, 25 °C) of (a) BPE^{2+} (5.0 mM), (b) **1** (2.0 mM) in the presence of 10.0 equiv of BPE^{2+}, (c) **1** (5.0 mM) in the presence of 1.0 equiv of BPE^{2+}, (d) **1** (5.0 mM), (e) MV^{2+} (5.0 mM) in the presence of 1.0 equiv of **1**, (f) **1** (2.0 mM) in the presence of 10.0 equiv of MV^{2+}, and (g) MV^{2+} (5.0 mM).

molecules. These changes of chemical shifts may be ascribable to the mutual diamagnetic shielding effect between guests and crown ether aromatic systems. Particularly, the proton signals of H_e on **1** gave a moderate downfield shift upon complexation with MV^{2+} ($\Delta\delta$ = 0.06 ppm, Figure 1b),[16] but the chemical shift of the same proton was almost unchanged for BPE^{2+} ($\Delta\delta$ = 0.01 ppm, Figure 1f). These observations are mainly attributed to the inductive effects of intermolecular C−H···O hydrogen bonds, which provides further evidence for the existence of hydrogen-bonding interactions between MV^{2+} and

dx.doi.org/10.1021/jp305503e | J. Phys. Chem. B 2012, 116, 9500−9506

polyether chains of **1**. Moreover, as compared to that induced by complex $BPE^{2+}\subset$**1**, it is noteworthy that the $\Delta\delta$ value induced by complex $MV^{2+}\subset$**1** was larger to some extent, indicative of a greater affinity in the complexation of **1** and MV^{2+}, which was further confirmed by their association constants (K_a) as described below. In addition, although it is well documented that MV^{2+} could form a supramolecular complex with precursor BMP26C8 in organic solution,[17] BMP26C8 could not interact with BPE^{2+} in acetonitrile due to the negligible complexation-induced chemical shifts in the ^{1}H NMR titration (Figure S11 of the Supporting Information). This result indicates that the introduction of negative charges can dramatically improve the binding abilities of crown ether **1** with BPE^{2+} in water.

Furthermore, Job's plot was performed to explore the binding stoichiometry of MV^{2+} and BPE^{2+} with **1**, in which the chemical shift of H_a on **1** versus the molar ratio showed an inflection point at a molar fraction of 0.5, revealing a 1:1 complexation stoichiometry in complexes $MV^{2+}\subset$**1** and $BPE^{2+}\subset$**1** (Figures S8 and S9 of the Supporting Information). After validation of the binding stoichiometry, the K_a values were calculated as 1.0×10^3 and 5.8×10^2 M^{-1} for $MV^{2+}\subset$**1** and $BPE^{2+}\subset$**1**, respectively, by analyzing the sequential changes in the chemical shift ($\Delta\delta$) of **1** upon the gradual addition of guest molecules, using a nonlinear least-squares curve-fitting method (Figure 2, inset).

Structure of Complexes. More direct evidence for the different binding behaviors was obtained from their single crystal in the solid state by the use of a vapor diffusion method, where each complex consists of one host and two guest molecules as their chemical formula to balance the intrinsic charge numbers, suggesting that the charge-matching molar ratio is the optimal condition in the formation of noncovalently constructed aggregates.

There are extensive intermolecular C−H···O hydrogen-bonding networks observed in the oxygen atoms of ethylene glycol chains on **1** and nitrogen atoms of MV^{2+} to stabilize the formation of the inclusion complex (Figure 3a). Moreover, as seen in Figure 3b, there are two original species of MV^{2+} in the packing structure of $MV^{2+}\subset$**1**; that is, one guest intermolecularly penetrates into the cavity of crown ether straight along the vertical direction to form [2]pseudorotaxane, whereas the other one is embedded in the crystal lattices as a counterion. The wheel **1** in the topologically interpenetrated structure adopts a Z-shape conformation, and two pyridinium rings in the axle MV^{2+} are approximately coplanar with an inclination angle of 8.9°. Furthermore, the centroid−centroid distances of aromatic rings in [2]pseudorotaxane were measured as 3.39 and 3.44 Å, respectively, ultimately resulting in $\pi-\pi$ stacking between the electron-rich sulfonated resorcinol rings of host **1** and the electron-deficient guest MV^{2+}. Aside from the $\pi-\pi$ stacking and hydrogen-bonding interaction, the ionic electrostatic attractions between the nitrogen atoms of pyridinium and the oxygen atoms of the sulfonate group ($d_{N1\cdots O10}$ = 4.16 Å, $d_{N1\cdots O12}$ = 3.48 Å, $d_{N2\cdots O15}$ = 3.88 Å, and $d_{N2\cdots O20}$ = 3.95 Å) jointly fix the geometric configurations of superstructure $MV^{2+}\subset$**1**.

Surprisingly, the complex $BPE^{2+}\subset$**1** exhibits different molecular binding and assembly behaviors in the solid state (Figure 4). Although the macrocycle of tetrasulfonated crown ether maintains a circular shape, there is no guest encapsulated in the cavity of the host, and four sulfonate units in **1** are surrounded by two BPE^{2+} molecules to form a tightly packed electrostatic complex, which is strikingly distinctive from the

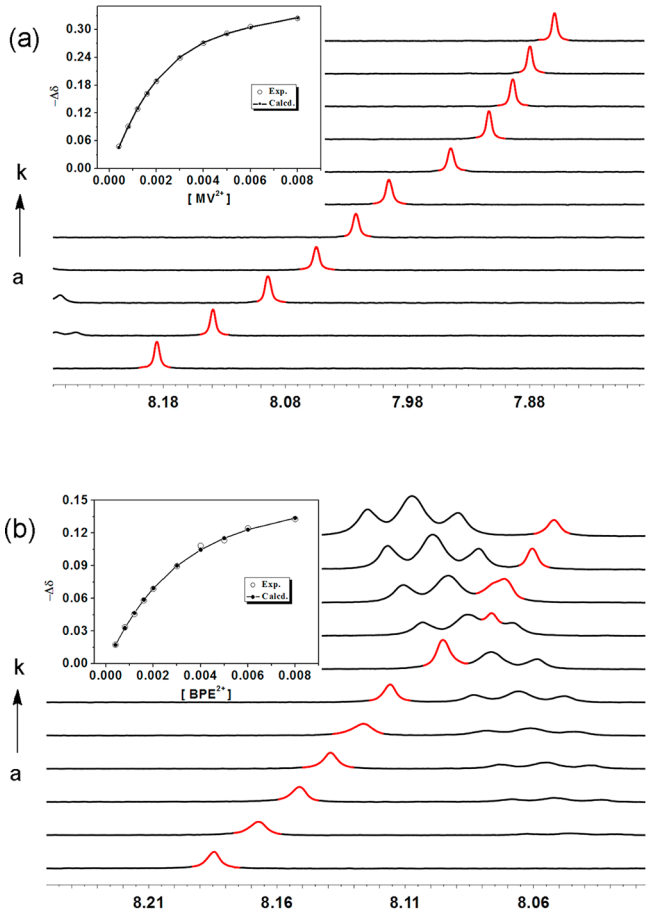

Figure 2. ^{1}H NMR spectral changes of **1** upon addition of (a) MV^{2+} and (b) BPE^{2+} in D_2O at 25 °C ([**1**] = 2.0 mM, $[MV^{2+}] = [BPE^{2+}]$ = 0, 0.4, 0.8, 1.2, 1.6, 2.0, 3.0, 4.0, 5.0, 6.0, and 8.0 M, from a to k, respectively). Inset: The nonlinear least-squares analysis of the differential chemical shifts ($\Delta\delta$) to calculate the association constant (K_a) for $MV^{2+}\subset$**1** and $BPE^{2+}\subset$**1**.

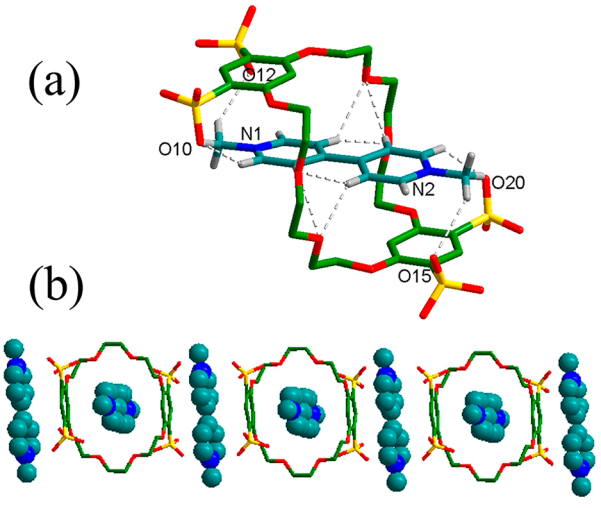

Figure 3. Crystal structures of (a) [2]pseudorotaxane and (b) the packing representation of $MV^{2+}\subset$**1**. Hydrogen-bond parameters are shown as follows: H···O distance (Å), C−H···O angle (deg), C···O distance (Å): 2.34, 158.1, 3.25; 2.95, 137.9, 3.71; 2.62, 152.2, 3.49; 2.45, 139.3, 3.23; 2.50, 147.9, 3.34; 2.47, 144.3, 3.32; 2.55, 136.2, 3.30; 2.83, 148.4, 3.70.

dx.doi.org/10.1021/jp305503e | J. Phys. Chem. B 2012, 116, 9500−9506

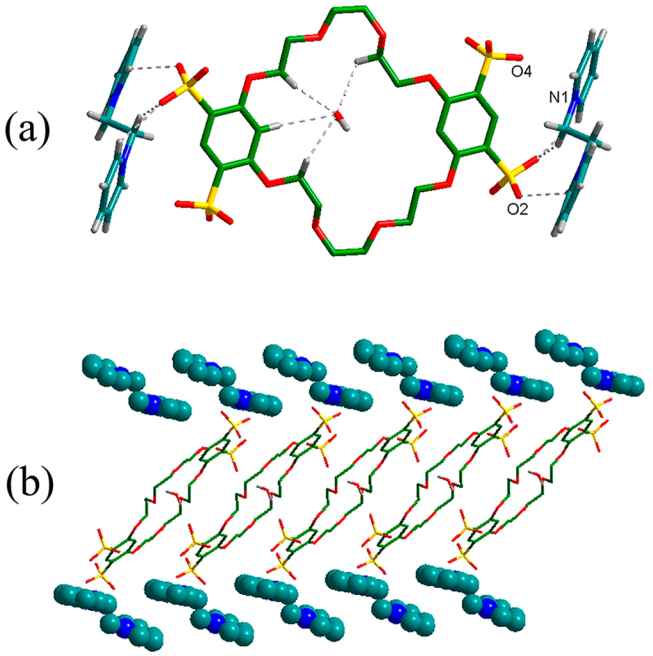

Figure 4. Crystal structures of (a) the electrostatic complex and (b) the packing representation of $BPE^{2+}\subset\mathbf{1}$. Hydrogen-bond parameters are shown as follows: H···O distance (Å), C−H···O angle (deg), C···O distance (Å): 2.77, 118.7, 3.36; 2.37, 129.6, 3.10; 2.67, 146.3, 3.60; 2.47, 135.2, 3.52.

interpenetrated structures of $MV^{2+}\subset\mathbf{1}$. The accurate measurement further demonstrates that the symmetrical distances between a pyridinium nitrogen atom and a sulfonate oxygen atom in $BPE^{2+}\subset\mathbf{1}$ are $d_{N1\cdots O2}$ = 3.24 Å and $d_{N1\cdots O4}$ = 3.69 Å, which are much closer than those in crystal $MV^{2+}\subset\mathbf{1}$. These strong ion−ion electrostatic attractions of the positively charged pyridinium units with the negatively charged benzene ring and few hydrogen-bonding interactions of C−H···O emerge to be the predominant forces in the formation of superstructure $BPE^{2+}\subset\mathbf{1}$. It should be noted that, in comparison to $MV^{2+}\subset\mathbf{1}$, one water molecule is constrained by four weak C−H···O hydrogen bonds in the cavity of **1**. This unexpected phenomenon indicates that BPE^{2+} has a weaker molecular complementarity toward the crown ether cavity.

Taking all the discussions into account, we reasonably infer that there are three principle aspects to illuminate the large disparities in these supramolecular arrays. As shown in Figure 5,

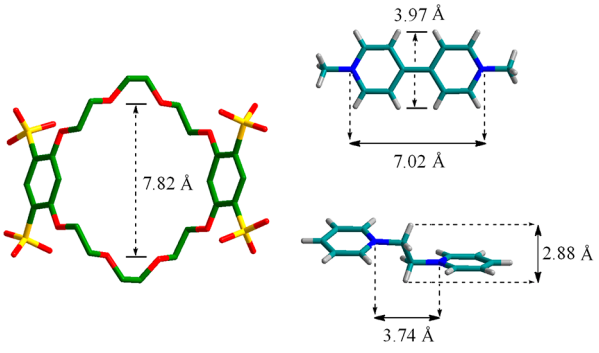

Figure 5. Molecular sizes measured from their corresponding crystal structures. (Macrocycle **1** was reproduced from the structure of $MV^{2+}\subset\mathbf{1}$, in which **1** has an unfolded ring.)

the intramolecular H−H width of MV^{2+} and BPE^{2+} is 3.97 and 2.88 Å, respectively, whereas the O−O distance of the unfolded ring **1** is 7.82 Å. As a result, the complex $MV^{2+}\subset\mathbf{1}$ may give a relatively greater size-fit efficiency, as compared with $BPE^{2+}\subset\mathbf{1}$, to form close contact of the C−H···O hydrogen bonds with the crown ether cavity. The conjugation of guest molecules is the second structural aspect responsible for the threading geometry of $MV^{2+}\subset\mathbf{1}$. Different from the flexible structure of BPE^{2+}, two pyridinium moieties in MV^{2+} are a cyclic π-aromatic system that increase its rigidity and delocalize the spin density on an atomic center. This π-conjugation makes MV^{2+} more electron deficient and, thus, leads to a stronger $\pi-\pi$ stacking interaction and less effective conformational loss upon the host−guest binding. Finally, the charge distribution can dramatically influence the complexation of **1** with guests. The N^+-N^+ interatomic distance of BPE^{2+} is 3.74 Å, which is much shorter than that of MV^{2+} (7.02 Å). The intensive positive charge on BPE^{2+} facilitates the close location between oppositely charged ionic components, while the diffusion of positive charges on MV^{2+} is unfavorable in the formation of an electrostatic complex with tetrasulfonated crown ether **1**.

Microcalorimetric Titration and Thermodynamics. Moreover, the molecular recognition process and thermodynamics of tetrasulfonated crown ether **1** with substrates were comparatively investigated in aqueous media by the method of isothermal titration calorimetry (ITC) measurements. The thermodynamic parameters are listed in Table S2 of the Supporting Information, in which K_a values are well-consistent with the ones obtained by ^{1}H NMR titrations. In the case of $MV^{2+}\subset\mathbf{1}$, the binding process is governed in a thermodynamically favorable way with negative enthalpy and positive entropy change, giving the following reliable thermodynamic parameters with reasonable errors: $\Delta G^\circ = -18.62 \pm 0.01$ kJ mol^{-1}, $\Delta H^\circ = -10.18 \pm 0.08$ kJ mol^{-1}, and $T\Delta S^\circ = 7.80 \pm 0.07$ kJ mol^{-1} (Figure 6). In contrast, as for the complexation of BPE^{2+} with **1**, it convincingly demonstrates that this binding process is strongly entropy driven, accompanied with a minimal enthalpic contribution ($\Delta G^\circ = -14.47 \pm 0.09$ kJ mol^{-1}, $\Delta H^\circ = -3.03 \pm 0.03$ kJ mol^{-1}, and $T\Delta S^\circ = 11.46 \pm 0.14$ kJ mol^{-1}, Figure 6). Meanwhile, for the purpose of comparison, the molecular binding behaviors between **1** and a bispyridinium salt with more flexible spacer, namely 1,4-bis(pyridinium)butane (BPB^{2+}), were further studied, and it is interesting to note that the corresponding chemical shift changes underwent the same tendency for BPE^{2+} and BPB^{2+} upon complexation with **1** (Figure S10 of the Supporting Information). Microcalorimetric experiments also showed that the thermodynamic behavior of complex $BPB^{2+}\subset\mathbf{1}$ was similar with that of $BPE^{2+}\subset\mathbf{1}$ in a favorably entropy-driven pathway (Table S2 and Figure S11 of the Supporting Information). The combined results demonstrate that the spacer flexibility in guest molecules can affect the binding mode of water-soluble crown ether **1** with bispyridinium cations.

These ITC data give more detailed information of the noncovalent interaction of **1** with guests and reinforce the aforementioned binding modes in the X-ray diffraction analyses. It is generally accepted that the noncovalent driving forces, such as hydrogen-bonding interconnection, $\pi-\pi$ stacking, and ion-dipole interactions in supramolecular assemblies, always lead to a positive contribution to enthalpy changes ($\Delta H^\circ < 0$), whereas the association process arising from ion−ion electrostatic attraction, conformational freedom, and the desolvation effect is entropically favored ($T\Delta S^\circ > 0$) in

dx.doi.org/10.1021/jp305503e | J. Phys. Chem. B 2012, 116, 9500−9506

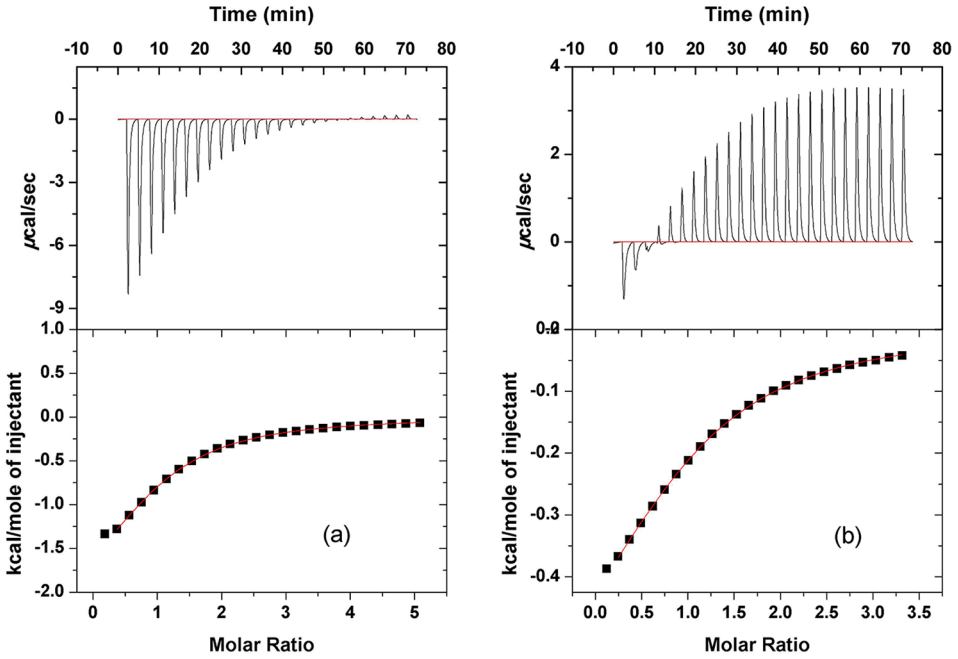

Figure 6. Calorimetric titrations of host **1** with MV^{2+} (a) and BPE^{2+} (b) in H_2O at 25 °C. Top: Raw data for sequential 10 μL injections of the guest solution (22.44 mM for MV^{2+} and 70.04 mM for BPE^{2+}) into the crown ether **1** solution (0.9055 mM for MV^{2+} and 4.033 mM for BPE^{2+}). Bottom: Heats of reaction as obtained from the integration of the calorimetric traces.

Scheme 2. Schematic Illustration of the Complexation of 1 with Guests To Form [2]Pseudorotaxane and the Electrostatic Complex

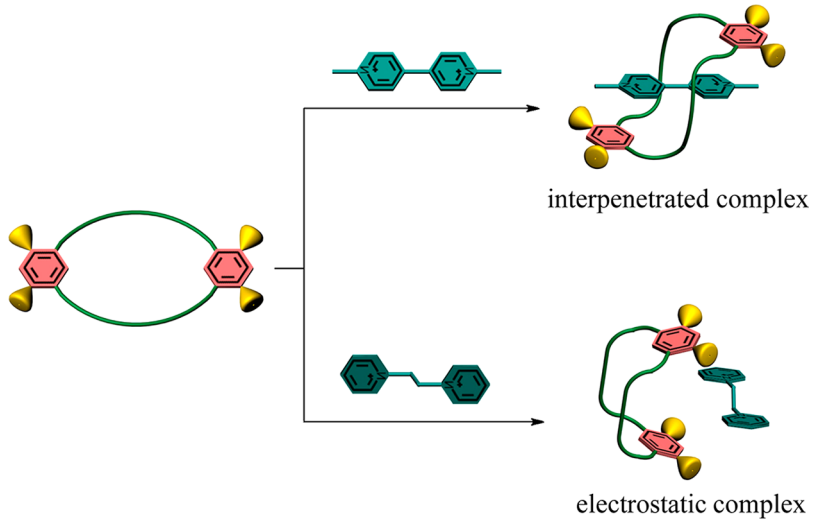

aqueous media.[18] In our case, the dominant enthalpy change indicates that the $N^+\cdots O^{\delta-}$ ion−dipole and the C−H···O hydrogen-bonding interconnection working at pyridinium moieties and ethylene glycol chains, as well as π−π stacking interactions of aromatic rings in [2]pseudorotaxane, play crucial roles for host−guest complexation of $MV^{2+}\subset$**1**. Although the incorporation of guest molecules makes the accommodated MV^{2+} structure more immovable in the crown ether cavity, the electrostatic and desolvation effect contribute to a large entropic gain, which overwhelm the entropic loss originating from the change of conformational freedom upon host−guest complexation. On the contrary, the entropy-controlled complexation indicates that the flexible guest BPE^{2+} mainly interacts with sulfonate groups on **1** to maximize the electrostatic attractions. Instead of ion−dipole, hydrogen bonds, and π−π stacking interactions in $MV^{2+}\subset$**1**, it can be rationalized that the electrostatic attraction and solvent reorganization are two major driving forces that govern the superstructure of $BPE^{2+}\subset$**1**. Combining the ^{1}H NMR experiment, crystallographic data, and ITC results, we can undoubtedly deduce that these two complexes could bind in a very different mode, as illustrated in Scheme 2.

CONCLUSION

In summary, a new tetrasulfonated crown ether **1** was synthesized and its thermodynamics−structure relationship with two organic cations, MV^{2+} and BPE^{2+}, was fully investigated in aqueous media and the solid state, producing the electrically interpenetrated structure and electrostatic complex for $MV^{2+}\subset$**1** and $BPE^{2+}\subset$**1**, respectively. The

dx.doi.org/10.1021/jp305503e | J. Phys. Chem. B 2012, 116, 9500−9506

introduction of four sulfonate groups onto the backbone of crown ether and the flexibility of linkers in guest molecules can profoundly affect the binding geometry and thus lead to the internal or external binding toward different cationic substrates. This structure-dependent complexation emphasizes that the utilization of electrostatic attraction in conjunction with other noncovalent interactions is highly desirable for the effective binding process in aqueous media. We also envision that the extension of our results may endow a variety of known crown ether derivatives with biocompatible properties and make water-soluble crown ether a promising candidate for applications in advanced functional nanodevices.

EXPERIMENTAL SECTION

Tetraethylammonium Bis(*m*-3,5-disulfonatepheny-lene)-26-crown-8 (2). A solution of chlorosulfonic acid (2.60 g, 22.30 mmol) in dry $CHCl_3$ (30 mL) was added dropwise to a stirred solution of bis(*m*-phenylene)-26-crown-8 (1.00 g, 2.23 mmol) in dry $CHCl_3$ (70 mL) at −5 °C over a period of 2 h. Then, the mixture was kept at −5 °C for an additional 4 h to give a white precipitate. The precipitate was carefully collected by filtration and washed at once with dry $CHCl_3$ (50 mL). The residue was taken up into H_2O (80 mL), and a NEt_4OH solution was added until the pH reached 7. The crude product was collected and dried in vacuo. After recrystallization three times from the acetonitrile−acetone mixtures and drying under a vacuum, the target compound was obtained as a white solid (2.14 g, 74.5%). Compound **2** has a tendency to absorb moisture from the humid air. ^{1}H NMR (400 MHz, D_2O): δ 8.24 (s, 2H, H_a), 7.05 (s, 2H, H_b), 4.51−4.42 (m, 8H, H_c), 4.03−3.95 (m, 8H, H_d), 3.83 (s, 8H, H_e), 3.29 (q, J = 7.3 Hz, 32H, $-NCH_2$), 1.38−1.20 (m, 48H, $-CH_3$). ^{13}C NMR (100 MHz, D_2O): δ 159.6, 128.9, 122.6, 100.6, 70.3, 69.4, 51.8, 6.5. HRMS (ESI): m/z calcd for $C_{40}H_{68}N_2O_{20}S_4$ $[M - 2NEt_4 + H]^-$, 1025.3325; found, 1025.3318. HRMS (ESI): m/z calcd for $C_{32}H_{49}O_{22}S_4$ $[M - 3NEt_4 + 2H]^-$, 896.1808; found, 896.1804.

Sodium Bis(*m*-3,5-disulfonatephenylene)-26-crown-8 (1). Compound **2** (1.00 g, 0.78 mmol) was dissolved in CH_3CN (30 mL), and a solution of $NaClO_4$ (1.31 g, 9.33 mmol) in CH_3CN (60 mL) was slowly added with stirring. The precipitate was filtered and washed three times with CH_3CN. After drying in vacuo, the anionic crown ether **1** was obtained as a white solid (0.65 g, 97.2%). ^{1}H NMR (400 MHz, D_2O): δ 8.19 (s, 2H, H_a), 6.98 (s, 2H, H_b), 4.40 (s, 8H, H_c), 3.93 (s, 8H, H_d), 3.77 (s, 8H, H_e). ^{13}C NMR (100 MHz, D_2O): δ 159.5, 128.9, 122.1, 100.2, 70.1, 69.1. HRMS (ESI): m/z calcd for $C_{24}H_{29}O_{20}Na_4S_4$ $[M + H]^+$, 856.9727; found, 856.9726. HRMS (ESI): m/z calcd for $C_{24}H_{31}O_{22}S_4$ $[M - 4Na + 3H]^-$, 767.0291; found, 767.0289.

Inclusion Complex of 1 with MV^{2+} ($MV^{2+}\subset$1). 1,1′-Dimethyl-[4,4′]-bispyridinium hexafluorophosphate in CH_3CN was added to a solution of **2** in CH_3CN, and a precipitate of $MV^{2+}\subset$**1** was formed at once. After filtration, a single crystal of $MV^{2+}\subset$**1** was grown by vapor diffusion of acetone into an aqueous solution of $MV^{2+}\subset$**1**. Crystal data for $MV^{2+}\subset$**1**: $C_{48}H_{80.8}N_4O_{32.40}S_4$, M = 1360.61, monoclinic, space group $P121/n1$, a = 14.825(2) Å, b = 19.659(3) Å, c = 21.761(4) Å, α = 90°, β = 95.970(4)°, γ = 90°, V = 6307.7(17) Å^3, $F(000)$ = 2880, Z = 4, D_c = 1.433 g cm^{-3}, μ = 0.245 mm^{-1}, and approximate crystal dimensions, 0.22 × 0.16 × 0.14 mm^3, θ range = 1.40−27.28°, 49613 measured reflections, of which 13983 (R_{int} = 0.0950) were unique. Final R indices $[I > 2\sigma(I)]$: R_1 = 0.1186, wR_2 = 0.3113. R indices (all data): R_1 = 0.1467, wR_2 = 0.3352, goodness of fit on F^2 = 1.095.

Electrostatic Complex of 1 with BPE^2 ($BPE^{2+}\subset$1). The crystal of $BPE^{2+}\subset$**1** was prepared via a procedure similar to that of $MV^{2+}\subset$**1**. Crystal data for $BPE^{2+}\subset$**1**: $C_{48}H_{58}N_4O_{21}S_4$, M = 1155.22, triclinic, space group $P\bar{1}$, a = 8.063(2) Å, b = 12.420(3) Å, c = 12.585(4) Å, α = 89.910(8)°, β = 86.228(10)°, γ = 82.075(10)°, V = 1245.5(6) Å^3, $F(000)$ = 606, Z = 1, D_c = 1.540 g cm^{-3}, μ = 0.279 mm^{-1}, approximate crystal dimensions, 0.20 × 0.18 × 0.12 mm^3, θ range =1.62−29.16°, and 13938 measured reflections, of which 6540 (R_{int} = 0.0281) were unique. Final R indices $[I > 2\sigma(I)]$: R_1 = 0.0402 and wR_2 = 0.1198. R indices (all data): R_1 = 0.0516, wR_2 = 0.1284, and goodness of fit on F^2 = 1.103.

ASSOCIATED CONTENT

Supporting Information

X-ray crystallographic data of $MV^{2+}\subset$**1** and $BPE^{2+}\subset$**1** in CIF format (CCDC No. 867553 and 867554, respectively). Characterization data for compounds **1** and **2**, chemical shift changes upon the complexation, Job's plots, thermodynamic parameters, as well as calorimetric titration curves. This material is available free of charge via the Internet at http://pubs.acs.org.

AUTHOR INFORMATION

Corresponding Author

*E-mail: yuliu@nankai.edu.cn.

Notes

The authors declare no competing financial interest.

ACKNOWLEDGMENTS

This work is financially supported by the 973 Program (2011CB932502), NNSFC (Grant 20932004), and the Fundamental Research Funds for the Central Universities (BE018201).

REFERENCES

(1) (a) Badjić, J. D.; Nelson, A.; Cantrill, S. J.; Turnbull, W. B.; Stoddart, J. F. *Acc. Chem. Res.* **2005**, *38*, 723−732. (b) Zhu, X.-Z.; Chen, C.-F. *J. Am. Chem. Soc.* **2005**, *127*, 13158−13159. (c) Loeb, S. J. *Chem. Soc. Rev.* **2007**, *36*, 226−235. (d) Wu, J.; Leung, K. C.-F.; Benítez, D.; Han, J.-Y.; Cantrill, S. J.; Fang, L.; Stoddart, J. F. *Angew. Chem., Int. Ed.* **2008**, *47*, 7470−7474. (e) Zheng, B.; Wang, F.; Dong, S.; Huang, F. *Chem. Soc. Rev.* **2012**, *41*, 1621−1636. (f) Zhang, Z.-J.; Zhang, H.-Y.; Liu, Y. *Chem. J. Chin. Univ.* **2011**, *32*, 1913−1927.

(2) (a) Balzani, V.; Credi, A.; Raymo, F. M.; Stoddart, J. F. *Angew. Chem., Int. Ed.* **2000**, *39*, 3348−3391. (b) Pease, A. R.; Jeppesen, J. O.; Stoddart, J. F.; Luo, Y.; Collier, C. P.; Heath, J. R. *Acc. Chem. Res.* **2001**, *34*, 433−444. (c) Korybut-Daszkiewicz, B.; Wieckowska, A.; Bilewicz, R.; Domagała, S.; Woźniak, K. *Angew. Chem., Int. Ed.* **2004**, *43*, 1668−1672. (d) Saha, S.; Stoddart, J. F. *Chem. Soc. Rev.* **2007**, *36*, 77−92. (e) Altobello, S.; Nikitin, K.; Stolarczyk, J. K.; Lestini, E.; Fitzmaurice, D. *Chem.—Eur. J.* **2008**, *14*, 1107−1116. (f) Dey, S. K.; Coskun, A.; Fahrenbach, A. C.; Barin, G.; Basuray, A. N.; Trabolsi, A.; Botros, Y. Y.; Stoddart, J. F. *Chem. Sci.* **2011**, *2*, 1046−1053. (g) Jiang, W.; Han, M.; Zhang, H.-Y.; Zhang, Z.-J.; Liu, Y. *Chem.—Eur. J.* **2009**, *15*, 9938−9945.

(3) (a) Cram, D. J.; Helgeson, R. C.; Peacock, S. C.; Kaplan, L. J.; Domeier, L. A.; Moreau, P.; Koga, K.; Mayer, J. M.; Chao, Y.; Siegel, M. G.; Hoffman, D. H.; Sogah, G. D. Y. *J. Org. Chem.* **1978**, *43*, 1930−1946. (b) Galán, A.; Andreu, D.; Echavarren, A. M.; Prados, P.; de Mendoza, J. *J. Am. Chem. Soc.* **1992**, *114*, 1511−1512. (c) van Nostrum, C. F.; Picken, S. J.; Nolte, R. J. M. *Angew. Chem., Int. Ed.*

1994, *33*, 2173−2175. (d) Gokel, G. W.; Leevy, W. M.; Weber, M. E. *Chem. Rev.* **2004**, *104*, 2723−2750.
(4) (a) Bu, J.-H.; Zheng, Q.-Y.; Chen, C.-F.; Huang, Z.-T. *Org. Lett.* **2004**, *6*, 3301−3303. (b) Liu, Y.; Han, M.; Zhang, H.-Y.; Yang, L.-X.; Jiang, W. *Org. Lett.* **2008**, *10*, 2873−2876.
(5) (a) Badjić, J. D.; Balzani, V.; Credi, A.; Silvi, S.; Stoddart, J. F. *Science* **2004**, *303*, 1845−1849. (b) Serreli, V.; Lee, C.-F.; Kay, E. R.; Leigh, D. A. *Nature* **2007**, *445*, 523−527. (c) Wang, F.; Han, C.; He, C.; Zhou, Q.; Zhang, J.; Wang, C.; Li, N.; Huang, F. *J. Am. Chem. Soc.* **2008**, *130*, 11254−11255. (d) Zhang, Z.-J.; Zhang, H.-Y.; Wang, H.; Liu, Y. *Angew. Chem., Int. Ed.* **2011**, *50*, 10834−10838.
(6) (a) Allwood, B. L.; Spencer, N.; Shahriari-Zavareh, H.; Stoddart, J. F.; Williams, D. J. *J. Chem. Soc., Chem. Commun.* **1987**, *14*, 1064−1066. (b) Gibson, H. W.; Wang, H.; Slebodnick, C.; Merola, J.; Kassel, W. S.; Rheingold, A. L. *J. Org. Chem.* **2007**, *72*, 3381−3393. (c) Han, T.; Chen, C.-F. *J. Org. Chem.* **2007**, *72*, 7287−7293. (d) Klivansky, L. M.; Koshkakaryan, G.; Cao, D.; Liu, Y. *Angew. Chem., Int. Ed.* **2009**, *48*, 4185−4189. (e) Zhang, M.; Zhu, K.; Huang, F. *Chem. Commun.* **2010**, 8131−8141.
(7) Gasa, T. B.; Valente, C.; Stoddart, J. F. *Chem. Soc. Rev.* **2011**, *40*, 57−78.
(8) Hoffart, D. J.; Tiburcio, J.; de la Torre, A.; Knight, L. K.; Loeb, S. J. *Angew. Chem., Int. Ed.* **2008**, *47*, 97−101.
(9) Lestini, E.; Nikitin, K.; Müller-Bunz, H.; Fitzmaurice, D. *Chem.—Eur. J.* **2008**, *14*, 1095−1106.
(10) (a) Liu, Y.; Chen, Y. *Acc. Chem. Res.* **2006**, *39*, 681−691. (b) Chen, Y.; Zhang, Y.-M.; Liu, Y. *Chem. Commun.* **2010**, 5622−5633.
(11) (a) Wang, K.; Guo, D.-S.; Zhang, H.-Q.; Li, D.; Zheng, X.-L.; Liu, Y. *J. Med. Chem.* **2009**, *52*, 6402−6412. (b) Guo, D.-S.; Chen, S.; Qian, H.; Zhang, H.-Q.; Liu, Y. *Chem. Commun.* **2010**, 2620−2622.
(12) (a) Liu, Y.; Shi, J.; Chen, Y.; Ke, C.-F. *Angew. Chem., Int. Ed.* **2008**, *47*, 7293−7296. (b) Zhang, Z.-J.; Zhang, Y.-M.; Liu, Y. *J. Org. Chem.* **2011**, *76*, 4682−4685.
(13) Lindsten, G.; Wennerstroem, O.; Isaksson, R. *J. Org. Chem.* **1987**, *52*, 547−554.
(14) Morzherin, Y.; Rudkevich, D. M.; Verboom, W.; Reinhoudt, D. N. *J. Org. Chem.* **1993**, *58*, 7602−7605.
(15) (a) Loeb, S. J.; Wisner, J. A. *Angew. Chem., Int. Ed.* **1998**, *37*, 2838−2840. (b) Elizarov, A. M.; Chiu, S.-H.; Stoddart, J. F. *J. Org. Chem.* **2002**, *67*, 9175−9181.
(16) More than 85% of the host **1** was associated with guests in both $MV^{2+}\subset$**1** and $BPE^{2+}\subset$**1** in the presence of 10.0 equiv of guest molecules.
(17) (a) Huang, F.; Gibson, H. W.; Bryant, W. S.; Nagvekar, D. S.; Froncze, F. R. *J. Am. Chem. Soc.* **2003**, *125*, 9367−9371. (b) Zhang, M.; Luo, Y.; Zheng, B.; Xia, B.; Huang, F. *Eur. J. Org. Chem.* **2010**, 5543−5547.
(18) (a) Bonal, C.; Israëli, Y.; Morel, J.-P.; Morel-Desrosiers, N. *J. Chem. Soc., Perkin Trans. 2* **2001**, 1075−1078. (b) Liu, Y.; Guo, D.-S.; Zhang, H.-Y.; Ma, Y.-H.; Yang, E.-C. *J. Phys. Chem. B* **2006**, *110*, 3428−3434. (c) Liu, Y.; Ma, Y.-H.; Chen, Y.; Guo, D.-S.; Li, Q. *J. Org. Chem.* **2006**, *71*, 6468−6473.